Optical constants of some silver alloys*

C. J. Flaten† and E. A. Stern
Department of Physics, University of Washington, Seattle, Washington 98195
(Received 21 August 1974)

The optical constants between 1.40 and 5.25 eV of three disordered alloy systems, AgCd, AgMg, and AgSn, have been directly measured over their respective α-phase ranges. The measurements indicate that the onset of the $L_2' - L_1$ transitions in pure Ag occurs at 3.33 ± 0.08 eV. The measurements clearly show the delineation of the alloys into two classes, one called class A, where the formalism of periodic structures with direct optical transitions is applicable, and one called class B, where this formalism is not applicable, and indirect optical transitions dominate in the changes caused by alloying. The plasma frequency in the Drude region is found to be a constant for these alloys within experimental error. For both of the class-A alloys, AgMg and AgCd, the electronic structure is very similar and a non-rigid-band variation of energy levels is found which can be qualitatively understood in terms of alloy theory. AgSn is a class-B alloy, the understanding of which is more difficult.

I. INTRODUCTION

Measurements of optical constants of pure solids and ordered compounds have been used to obtain important information on their electronic structure. Optical measurements on disordered alloys also contain valuable information but the full exploitation of this information requires a greater understanding of the electronic properties of disordered solids than is presently available. Only in the simpler alloy systems is there any hope of interpreting the measurements in a manner to elucidate the basic electronic structure.

The simplest alloys are those that can be treated by perturbation theory.[1] For such alloys the difference in the effective potential or pseudopotential between the constituents of the alloy is small compared to bandwidth energies. In practice, such conditions are usually satisfied for isovalent (same valence) constituents or for constituents whose difference in valence is small compared to the number of electrons per atom required to fill the overlapping bands.

The next simplest class of alloys is the so-called forward-scattering one[2] where the scattering perturbation introduced by replacing one type of atom by another has a much larger diagonal matrix element in a basis of Bloch states than the average nondiagonal element.

In both these classes of alloys, the qualitative ideas of pure crystalline materials are applicable and all of the insights available for pure materials can also be utilized for these alloys.[2,3] For example, the concepts of k space, energy bands, energy versus $\vec{k}$ relations, and the Fermi surface all can be used for these alloys with suitable smearing of the $E(k)$ relation. We will denote both of these classes of alloys as class-A alloys.[4] The characteristic of class-A alloys most pertinent for optical data is that the absorptions are dominated by $\vec{k}$-conserving (direct) transitions.

The alloys which cannot be classified as class-A alloys because their scattering is too great we will denote by class-B alloys.[4] The description of such alloys is not presently known for the general case. Progress has been made to calculate some of their properties but the models used have been too idealized to describe reality.[5] The relation of optical properties to the electronic structure of such class-B alloys therefore will be more difficult to ascertain than for class-A alloys. The characteristic of class-B alloys most pertinent for optical data is that *changes* in absorption cannot be described by direct transitions. In fact, the concept of an $E(\vec{k})$ relation to describe changes in optical absorption has no validity.

In this paper we investigate the optical properties of silver-based α-phase alloys. Two of the alloys, AgMg and AgCd, are class-A alloys for that portion of their energy bands that are mainly s-p character. The d-band dominant part of the electron structure of those alloys is class B. The third alloy system studied is the α-phase of AgSn. This alloy is class B throughout its whole range.

In class-A alloys the forward-scattering ones are more interesting than the perturbation ones because the possible changes on alloying are richer in scope. For example, large changes in z, the electron per atom ratio, can occur in forward-scattering alloys and not in perturbation ones. AgMg and AgCd are forward-scattering alloys in their class-A behavior.

Other noble-metal-based alloys can also be classified into A or B but the variations of optical absorption with composition are not so striking as for silver-based alloys. In addition, the transitions that contribute to the structure in the Ag absorption is less controversal than for the other noble metals. Temperature dependence of the optical constants,[6] alloying studies,[7,8] and piezo-

optical studies[9–11] have permitted a unique assignment to these transitions. Previous studies on Ag-based alloys have been made on AgPd,[12] AgAu,[13] AgAl,[8] AgZn,[7] AgCd,[7] and AgIn.[10,14] The results of these studies are consistent with the *A* and *B* classification discussed here.

An extensive study of Cu-based alloys was made by Pells and Montgomery[15] which tentatively suggested that in some alloys direct transitions dominate while in others indirect transitions are dominant. We will show that, in a more striking and convincing manner, such is also the case for Ag-based alloys and will show that both the Cu-based and Ag-based alloy behavior can be understood quantitatively in terms of the idea of class-*A* and class-*B* alloys. Class-*A* or -*B* behavior can be determined independent of the optical data, and the optical data are found consistent with this classification.

Another important new result from the measurements relates to the onset of interband transitions for pure Ag. The measured value of the onset of interband transitions is 3.33 ± 0.08 eV, in excellent agreement with the value of the relativistic calculations of Christensen[16] of 3.37 eV. This onset is of the order of 1 eV smaller than previously ascertained. Other new results are discussed in the body of the paper.

Mg and Cd were chosen as alloying elements to probe the different perturbation of the alloy *d* band caused by them. Cd has an occupied *d* band while Mg has no occupied one. It was found that within experimental error, they perturb the *d* band of Ag the same. This offhand surprising result is in agreement with alloy theory.

Section II presents the experimental details. Section III presents the experimental results. A review of the ideas of alloy theory used in interpretation of the data is given in Sec. IV. An analysis of the experimental data is presented in Sec. V. Section VI consists of a discussion, and a summary and conclusions are presented in Sec. VII.

II. EXPERIMENTAL DETAILS

Only a brief outline of the experimental details will be presented here. Full details are presented in Ref. 17. The optical constants were directly measured by a Drude method over the photon interval of 1.40–5.25 eV. The ellipsometer used in the measurement was automated to greatly facilitate the accumulation of the large amount of data obtained.

Alloy samples were prepared by simultaneous vacuum evaporation of the two constituents by an electron beam in a controlled fashion so that the ratio of the evaporated components remained constant throughout the evaporation. The substrates were glass microscope slides cleaned by standard techniques and outgassed at 200 °C for several hours in $10^{-7} - 10^{-6}$-Torr vacuum before cooling to 100 °C, at which time the sample was evaporated *in situ* at pressures that typically did not rise above 2×10^{-6} Torr. The samples, typically several thousand angstroms in thickness were then cooled to room temperature in vacuum before being taken out into the air where measurements were made. The effects of contaminants were checked by seeing if any change in the measured optical constants occurred between the time when measurements were started, typically within a few hours after exposure to air, and after periods up to several months of storage in a desiccator. Deterioration was noticeable only after several months leading us to believe that contaminants had a negligible effect on the measurements.

Alloy concentrations were determined by the position of the (111) x-ray diffraction peak. Uncertainty in locating the position of the peak introduced uncertainties in the composition of 1% for AgCd, 2.5% for AgMg, and 0.5% for AgSn. As was determined by a careful assessment,[18] other uncertainties in composition were introduced by variations in the (111) diffraction peak caused by sample defects and occluded gases. These introduced additional uncertainties in composition of AgCd alloys of ±3% and presumably similar uncertainties for AgMg alloys.

The experimental inaccuracies in the optical constants were carefully assessed and are indicated in Table I. These are absolute errors. The relative errors are smaller. The light wavelength was determined by a Jarrell-Ash $\frac{1}{4}$-m monochromater with a typical resolution of 50 Å. Possible problems from stray light and second-order light were carefully guarded against.

III. EXPERIMENTAL RESULTS

The experimental results for the real and imaginary parts, ϵ_1 and ϵ_2, respectively, for pure Ag are shown in Figs. 1 and 2, respectively. Our measurements are shown by the solid line while

TABLE I. Estimates of experimental errors.

Energy (eV)	ϵ_1	ϵ_2 (%)
1.50	±3%	±9
1.75	±2%	±7
2.00	±2%	±5
2.25–2.75	±2%	±3
3.00–3.50	±2%	±2
3.75	±0.04[a]	±2
4.0–5.25	±0.06[a]	±2

[a]These errors in ϵ_1 are given as absolute values since in this region ϵ_1 may be close to zero and the fractional error is not a good measure.

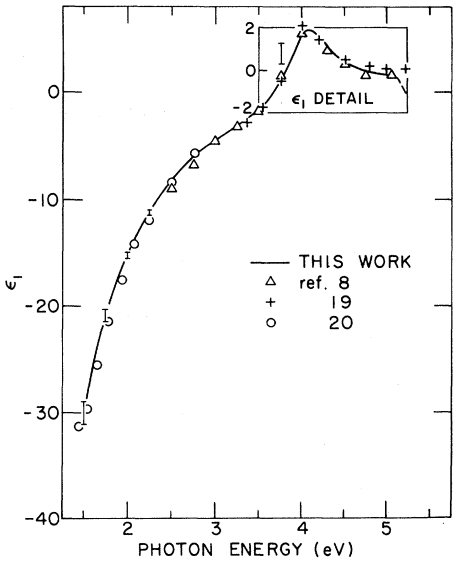

FIG. 1. Real part of the dielectric constant ϵ_1 for pure Ag as a function of photon energy. The results of this paper are indicated by the solid curve with errors indicated by the vertical error bars. For comparison, the results of Huebner *et al.* (Ref. 19) are shown by the symbol +; those of Irani *et al.* (Ref. 8) by the symbol Δ; and those of Schulz (Ref. 20) by the symbol o.

the results of other investigations[8,19,20] are shown by variously shaped points. In general, the agreement is good, giving confidence in our experimental technique and verifying that contamination is

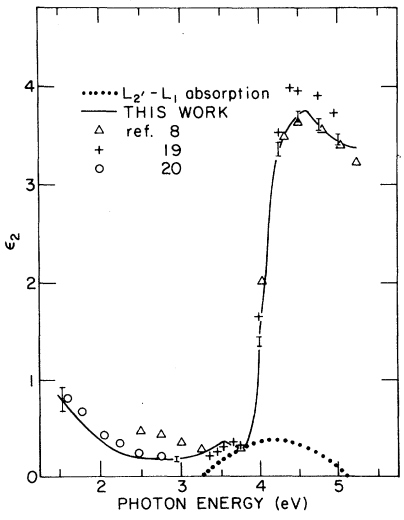

FIG. 2. Imaginary part of the dielectric constant ϵ_2 for pure Ag as a function of photon energy. The results of this paper are indicated by the solid curve with errors indicated by the vertical error bars. For comparison, the results of Huebner *et al.* (Ref. 19) are shown by the symbol +; those of Irani *et al.* (Ref. 8) by the symbol Δ; and those of Schulz (Ref. 20) by the symbol o.

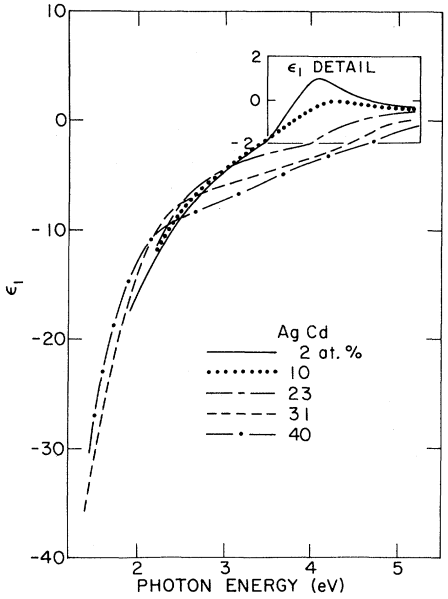

FIG. 3. Real part of the dielectric constant ϵ_1 for some α-phase AgCd alloys as a function of photon energy. The results are shown for the following atomic percentages of Cd: 2 at.%, solid line; 10 at.%, dotted line; 23 at.%, long-short dashed line; 31 at.%, dashed line; 40 at.%, dot-dashed line. The errors are of the same order as indicated for pure Ag in Fig. 1.

not important since, for example, Irani *et al.*[8] measured reflectivity in ultrahigh vacuum and used a Kramers-Kronig inversion to obtain the optical constants.

The values of ϵ_1 and ϵ_2 for α-phase AgCd alloys are presented in Figs. 3 and 4, respectively. The results agree qualitatively with those of Green and Muldawer.[7] The most obvious difference occurs in the low-energy region where the Drude tails of our data vary with composition while those of Green and Muldawer do not. We believe that the Drude tails as measured by Green and Muldawer are not reliable since they arbitrarily normalized the reflectance data of all of their samples to be equal to 0.91 at low energy. Their optical constants were obtained by Kramers-Kronig analysis of reflectance data and their arbitrary normalization procedure fixed the equality of the Drude tails at low energy. We find from our measurements a reflectivity at low energy (1.50 eV) varying from 0.99 for pure Ag to 0.95 for 40-at.% Cd in Ag. The arbitrary normalization will quantitatively affect the behavior of the Green-Muldawer data throughout the whole range, though not their qualitative behavior.

The values of ϵ_1 and ϵ_2 for α-phase AgMg alloys are presented in Figs. 5 and 6, respectively. To our knowledge there are no other measurements with which to compare. The variations measured

in the AgMg alloys is quite similar to those in AgCd as will be discussed in more detail later on.

The values of ϵ_1 and ϵ_2 for α-phase AgSn are shown in Fig. 7. The variations with composition are qualitatively strikingly different from AgMg and AgCd. Again, to our knowledge, there are no other measurements with which to compare.

IV. THEORETICAL CONSIDERATIONS

The concepts of pure metals such as Bloch states, energy bands, energy gaps at Brillouin zone boundaries, Fermi surfaces, etc., all are rigorously valid only in a periodic potential as in pure perfect single-crystal metals. Thus, one must question whether these concepts have any applicability to disordered alloys. An analysis of this problem[2,3] shows that one can classify disorder in alloys into at least two types, denoted by class A and class B.[4] In class-A disordered alloys the disorder is weak enough so that all of the concepts of pure materials are still good approximations. In class-B disordered alloys the disorder is strong enough so that the concepts of pure materials are limited to describing only some properties in the dilute range. Actual alloys cover the spectrum of disorder from the one extreme of class A to the other extreme of class B in a more or less continuous fashion so that there are alloys

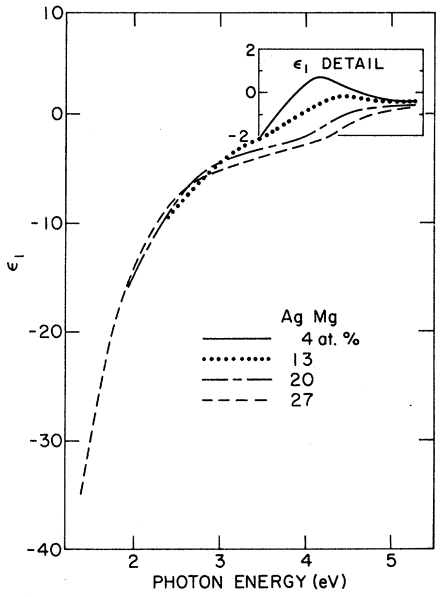

FIG. 5. Real part of the dielectric constant ϵ_1 for some α-phase AgMg alloys as a function of photon energy. The results are shown for the following atomic percentages of Mg: 4 at.%, solid line; 13 at.%, dotted line; 20 at.%, long-short dashed line; 27 at.%, dashed line. The errors are of the same order as indicated for pure Ag in Fig. 1.

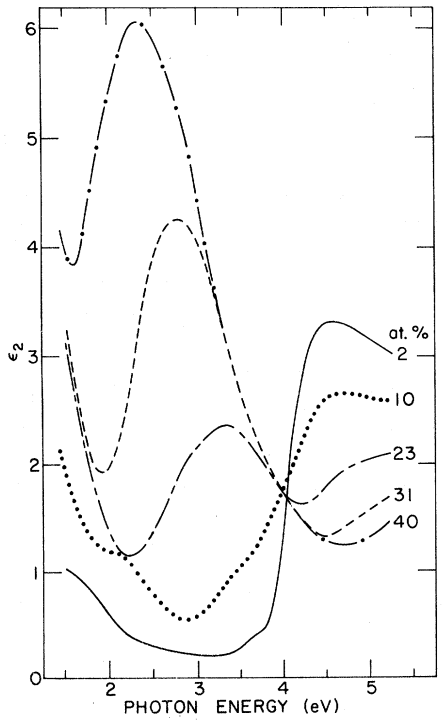

FIG. 4. Imaginary part of the dielectric constant ϵ_2 for some α-phase AgCd alloys as a function of photon energy. The results are shown for the following atomic percentages of Cd: 2 at.%, solid line; 10 at.%, dotted line; 23 at.%, long-short dashed line; 31 at.%, dashed line; 40 at.%, dot-dashed line. The errors are of the same order as indicated for pure Ag in Fig. 2.

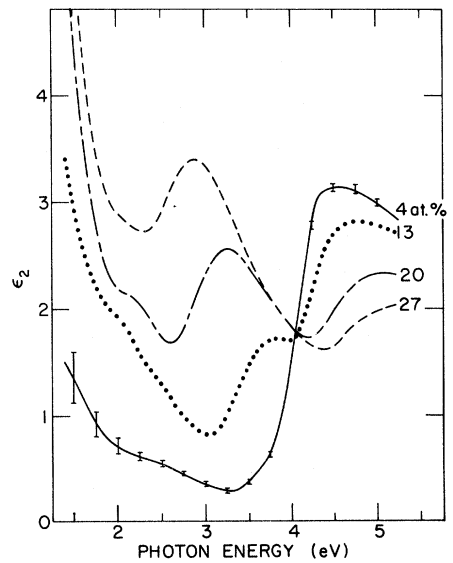

FIG. 6. Imaginary part of the dielectric constant ϵ_2 for some α-phase AgMg alloys as a function of photon energy. The results are shown for the following atomic percentages of Mg: 4 at.%, solid line; 13 at.%, dotted line; 20 at.%, long-short dashed line; 27 at.%, dashed line. The errors are of the same order as indicated for pure Ag in Fig. 2.

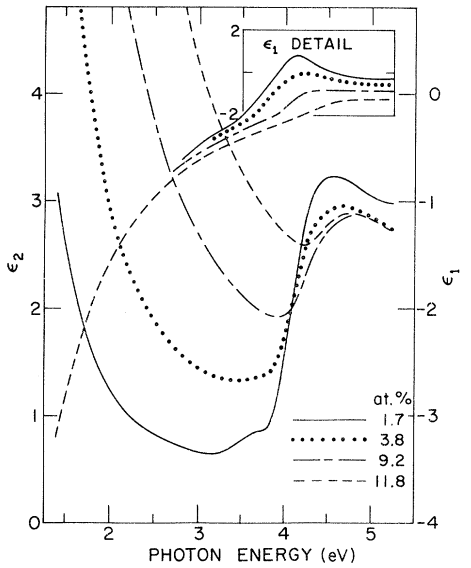

FIG. 7. Real and imaginary parts of the dielectric constant ϵ_1 and ϵ_2, respectively, for some α-phase AgSn alloys as a function of photon energy. The results are shown for the following atomic percentages of Sn: 1.7 at.%, solid line; 3.8 at.%, dotted line; 9.2 at.%, long-short dashed line; 11.8 at.%, dashed line. The errors for ϵ_1 and ϵ_2 are of the same order as indicated for pure Ag in Figs. 1 and 2, respectively.

which do not fit uniquely in one class or the other. The measure of the disorder, whether weak or strong, is not determined by the concentration of the second component. Even in dilute alloys it is possible to distinguish between weak and strong disorder.

Any alloy that can be treated by perturbation theory is automatically a type-*A* alloy. We turn to those alloys which cannot be treated by perturbation theory. To understand the distinction between class-*A* and class-*B* disorder consider a dilute alloy. The impurities in the alloy will scatter the eigenstates of the pure host. This scattering is the mechanism for the increase in electrical resistance caused by the impurities. This scattering produces a finite lifetime to the original eigenstates which can be described by adding a small imaginary part to the energy of the state making it complex.[2-4] Besides adding an imaginary part to the energy, the impurities also change the real part of the energy because they modify the potential felt by the electrons. If the complex energy in the dilute alloy of an original Bloch state $|\vec{k}\rangle$ is denoted by $E(\mathrm{k})$, then, from our previous discussion, we can write

$$E(\vec{k}) = E_0(\vec{k}) + \Sigma(\vec{k}), \tag{1}$$

where $E_0(\vec{k})$ is the energy of $|\vec{k}\rangle$ in pure host and

$$\Sigma(\vec{k}) = \Sigma_1(\vec{k}) + i\Sigma_2(\vec{k}). \tag{2}$$

Here $\Sigma_1(\vec{k})$ and $\Sigma_2(\vec{k})$ are the real and imaginary parts of $\Sigma(\vec{k})$, respectively.

We can define the two classes of disorder in terms of $\Sigma_1(\vec{k})$ and $\Sigma_2(\vec{k})$. In class-*A* alloys, in the region of interest,[2-4]

$$x^2 \equiv \left|\frac{\Sigma_2(\vec{k})}{\Sigma_1(\vec{k})}\right| \ll 1. \tag{3}$$

In class-*B* alloys, in the region of interest,[2-4]

$$x^2 \gtrsim 1. \tag{4}$$

In class-*A* alloys, changes in the shape of the Fermi surface with alloying can be defined. These changes follow approximately the prescription of the rigid-band model. In fact, the concepts of the rigid-band model are valid if one uses $E_0(\vec{k}) + \Sigma_1(\vec{k})$ in place of the energy values of the pure host $E_0(\mathrm{k})$. In addition, all the other concepts of pure materials are valid if one again replaces $E_0(\mathrm{k})$ by $E_0(\vec{k}) + \Sigma_1(\vec{k})$. The Boltzmann equation can be used to describe the motion of electrons in the class-*A* alloys under electromagnetic fields where the same scattering mechanisms that produced $\Sigma_2(\vec{k})$ are to be put into the equation. In particular, all the equations derived for pure materials are also valid for class-*A* alloys.[2,3] As an example, the Fermi surface is that constant energy surface

$$E_0(\vec{k}) + \Sigma_1(\vec{k}) = E_f, \tag{5}$$

which encloses a volume of k space containing the correct number of electrons per atom. The number of electrons per atom is, in the cases to be considered in this paper though not in all cases, given by the average number of valence electrons per atom. Thus, as the electron per atom ratio increases by alloying, the volume of the Fermi surface also expands. These results are not limited to dilute alloys but are valid for all concentrations of class-*A* alloys.

The condition (3) for type-*A* alloys can be interpreted[2-4] to mean that the variation in the Fermi surface with alloying is such that the *change* of the dimensions in k space is much larger than the smearing. Condition (3) also guarantees that the Fermi surface remains well defined for all alloy concentrations.

In class-*B* alloys, changes in the shape of the Fermi surface can no longer be uniquely defined, even in the dilute case. In the concentrated range, a Fermi surface is no longer a useful concept in class-*B* alloys. The Fermi surface is so smeared out that it no longer exists. In the dilute limit the Fermi surface, of course, exists for class-*B* alloys, but *changes* in the electronic properties induced by alloying can no longer be described in terms of the concepts of pure materials. For example, changes in the optical absorption of photons with alloying cannot be described in terms of tran-

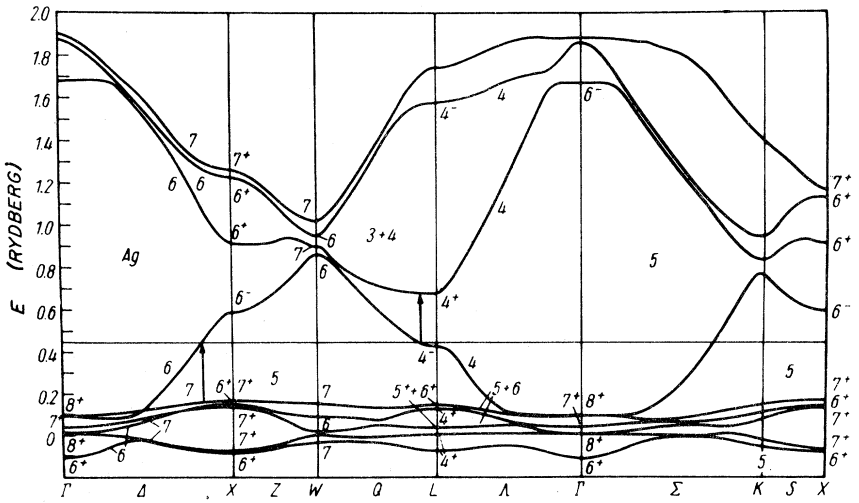

FIG. 8. Band structure for pure Ag along symmetry lines as calculated by Christensen (Ref. 16) by the relativistic augmented-plane-wave method. The transitions that cause the onset of absorption between bands 5 and 6 and between bands 6 and 7 are shown by the vertical arrows. Energies are in rydbergs above the muffin-tin zero.

sitions that conserve crystal momentum $\vec{k}$ as can be done for class-*A* alloys or pure materials. How to describe the electronic properties of concentrated class-*B* alloys is still an open question, not fully answered.

In Fig. 8 we present the energy-band calculation of Christensen[16] for pure Ag using the relativistic-augmented-plane-wave (RAPW) method. The notation differs from the more common nonrelativistic notation and the connection between the two is given in Table II for the *L* point, the one of most interest to us here. We will require this band structure to interpret the data. The rigid band model of alloys assumes that this energy structure is still valid in the alloy and the only effect of alloying is to cause E_f to rise to accommodate the increase in the electron per atom ratio z.

V. ANALYSIS OF DATA

The most striking aspect of the data in Figs. 1–7 is the similarity between AgMg and AgCd alloys and their difference from AgSn. In AgMg and AgCd the absorption onset in ϵ_2 near 4 eV for pure Ag splits into two peaks—one decreasing, the other increasing in energy as the z of the alloy increases. As pointed out by previous investigations,[6–11] this behavior can be understood as transitions between bands 5 and 6 and bands 6 and 7 as indicated by the arrows in Fig. 8. The bands are counted from the bottom up. The separation of the absorption peaks with alloying is qualitatively understood on the basis of the rigid model. As z increases, so does E_f, decreasing the energy of transitions from band 6 to 7 and increasing that of transitions from band 5 to 6. Thus, the lowering peak should be associated with transitions near $L_2' \rightarrow L_1$ and the rising peak should be associated with transitions from the top of the *d* band to E_f. This assessment agrees with that of the previous investigations.

To permit quantitative measurement of the variation of these interband peaks with concentration, one must subtract out the contribution from the intraband absorption or the Drude tail. For AgMg and AgCd the low-energy values of ϵ_1 and ϵ_2 can be closely approximated by the Drude form

$$\epsilon_1 = \epsilon_1^0 - \omega_p^2\tau^2(\omega^2\tau^2+1)^{-1},$$
$$\epsilon_2 = \omega_p^2\tau/\omega(\omega^2\tau^2+1), \tag{6}$$

where ω is the angular frequency of the incident light, τ is the relaxation time of the electrons, and $\omega_p = 4\pi ne^2/m^*$ is the plasma frequency. Here m^* is the effective mass of the electrons and n is the numbers of conduction electrons per unit volume.

The values of the parameters one obtains from this fitting are shown in Figs. 9–11. As shown in Fig. 9 the values obtained for $E_p = \hbar\omega_p$ are, surprisingly, a constant independent of concentration. This implies that n/m^* is a constant throughout the α-phase. For comparison, E_p for the β'-ordered phase of AgMg is also shown in Fig. 9. The value for E_p varies with the phase of the alloy. Also shown for comparison is the expected variation of E_p with z if m^* were a constant. There are slight differences expected in this variation of E_p between AgMg, AgCd, and AgSn due to different volume changes on alloying but these are at most 3.2% at $z = 1.4$. It is clear that m^* is varying significantly

TABLE II. Comparison between relativistic and nonrelativistic notation.

Nonrelativistic	Relativistic
L_2'	L_4^-
L_3	$L_{5^+6^+}$
L_1	L_4^+

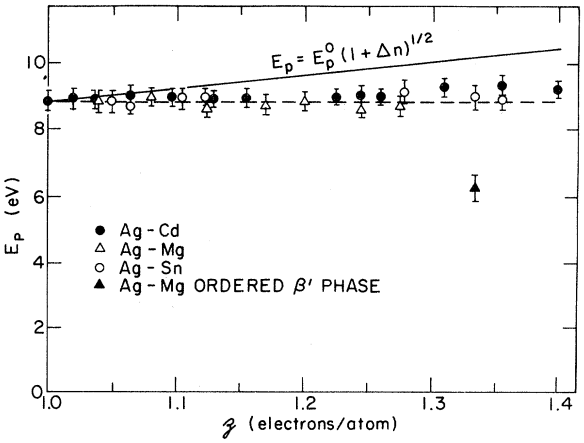

FIG. 9. Plasma energy in the Drude region for α-phase AgCd, AgMg, and AgSn as a function of electron per atom ratio $\mathcal{Z}$. One point for an ordered β'-phase of AgMg is also shown.

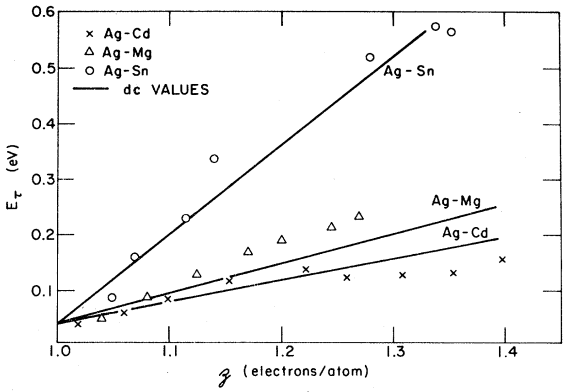

FIG. 11. Energy $E_\tau = \hbar/\tau$ associated with the relaxation lifetime of electrons in various α-phases of Ag-based alloys as a function of electrons per atom $\mathcal{Z}$. The dc values are slopes obtained from residual-resistance changes in dilute alloys.

in order to maintain E_p constant.

The values of ϵ_1^0 are presented in Fig. 10 while values of $E_\tau = \hbar/\tau$ are shown in Fig. 11. For comparison, the increase in E_τ predicted by the measured increase in residual dc resistance in dilute alloys is also shown. The relative scattering strengths of Mg, Cd, and Sn in Ag are the same at optical frequencies as they are at dc. Table III shows the comparison between some of the Drude parameters as measured by various investigators[6,20–23] for pure Ag.

Subtracting the Drude tail from the experimental data of ϵ, one obtains the interband contribution. A typical example is shown in Fig. 12 for ϵ_2 for a 25-at.% AgMg alloy. The two interband peaks near 3 and 5 eV are visible as is another peak around 2.2 eV. This low-energy peak is not interpreted as an interband transition because, in contrast to the two interband absorptions, it is strongly dependent on the conditions under which the sample was made such as substrate temperature, evaporation rate and residual gas pressure. This low-energy peak usually appears near 2.5 eV and is visible in dilute AgCd and in most of the AgMg alloys. The absorption is not related to oxide layers on the surface of the sample as studies of samples aged for two months and of pure magnesium have shown. The likely explanation for this low-energy peak is film imperfections. Measurements[24] on Ag films have shown that introducing structural disorder by evaporating on a 140 °K substrate produces an absorption peaked at 2.4 eV, while measurements[22] on poorly crystallized films produced at room temperature showed an anomalous absorption peaked at about 1.5 eV. In our further discussions in this paper we eliminate the effects of this anomalous peak and neglect them.

At large concentration, the low-energy interband peak is well separated from the high-energy peak and it is possible to accurately plot the onset energy of this absorption and its peak as a function of concentration. The onset energy was defined as

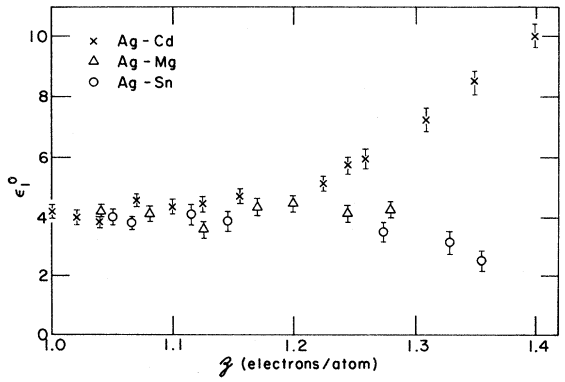

FIG. 10. Static ion-core contribution to the real part of the dielectric constant ϵ_1^0 for various α-phases of Ag-based alloys as a function of electrons per atom $\mathcal{Z}$.

TABLE III. Comparison of Drude parameters at room temperature for pure Ag as measured by various investigations.

Investigation	E_p (eV)	m^* [a]	τ (sec)
This work	8.85 ± 0.2	1.02 ± 0.05	$1.8 \pm 0.3 \times 10^{-14}$
Ref. 21	8.81 ± 0.3	1.03 ± 0.06	$3.7\text{-}1.6 \times 10^{-14}$
Ref. 23	9.12 ± 0.2	0.96 ± 0.04	$3.1 \pm 1.2 \times 10^{-14}$
Ref. 22	9.67 ± 0.06	0.87 ± 0.01	1.75×10^{-14}
Winsemius[b]	8.75	1.06	0.86×10^{-14}

[a] In units of the free-electron mass.
[b] Reference 6b.

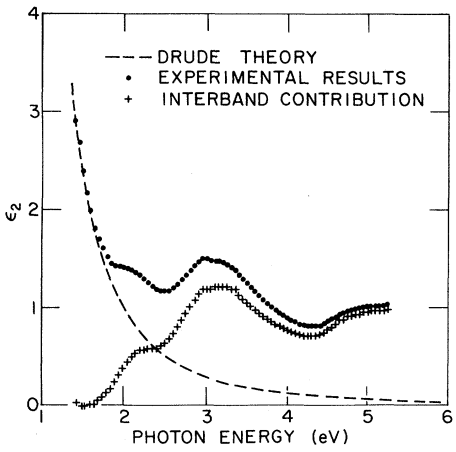

FIG. 12. Decomposition of ϵ_2 into interband and intraband (Drude) parts for a 25 at.% Mg in Ag α-phase alloy.

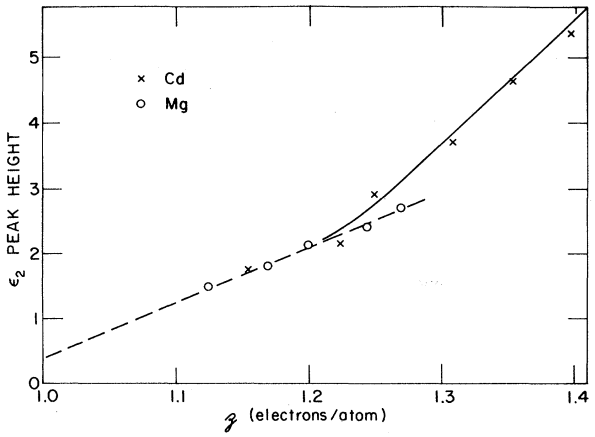

FIG. 14. Dependence of the ϵ_2 peak height of the low-energy absorption as a function of electron per atom ratio $\mathcal{g}$ for α-phase AgMg and AgCd.

that energy where the maximum slope on the low-energy side of the absorption intersects the energy axis. The plot of the onset energy and peak as a function of concentration is shown in Fig. 13. It is noted that the width of the absorption peak is approximately independent of concentration.

The extrapolation to pure Ag is well defined and surprising in its value for the onset of 3.33 ± 0.08 eV. This onset is much lower than previously measured and requires some explanation. The explanation is dependent on the variation of the peak height of this absorption with concentration as shown in Fig. 14. Extrapolating to pure Ag one notes that the peak height is quite small. The predicted contribution of this absorption to pure Ag is plotted by the dotted curve in Fig. 2 and we immediately see why it was not noted in measurements on pure Ag. The onset is very weak and overlaps the region where surface plasmons contribute an absorption which varies with sample preparation.[25,26] Yet, in hindsight, one sees evidence for this onset in previous measurements. Piezooptical measurements[10,11] in pure Ag show beginning of structure of the L_2'-L_1-type transition at a value consistent with the 3.33-eV value measured here but the authors did not quote the onset energy. Wavelength-modulated reflectivity measurements[27] also indicated some structure around 3.3 eV, which was attributed to surface plasmons. Careful photoemission studies[28] and recent temperature-modulated reflectance studies[29] have addressed themselves to the value of the $L_2' \rightarrow L_1$ onset energy and have obtained values of 3.8 eV or higher. The discrepancy between these results and ours appears to be real and its cause is unknown. One highly unlikely possibility is the linear extrapolation used here to obtain the onset energy may break down at low concentrations.

In Fig. 15 we show a plot of the energy at which the second derivative of ϵ_2 for the high-energy peak

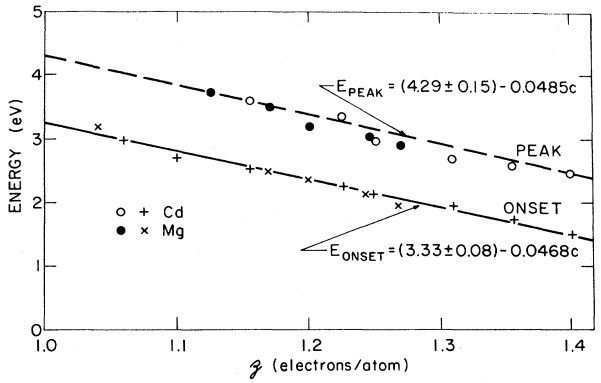

FIG. 13. Variation of the ϵ_2 peak and onset energies of the low-energy absorption as a function of electron per atom ratio $\mathcal{g}$ for α-phase AgMg and AgCd.

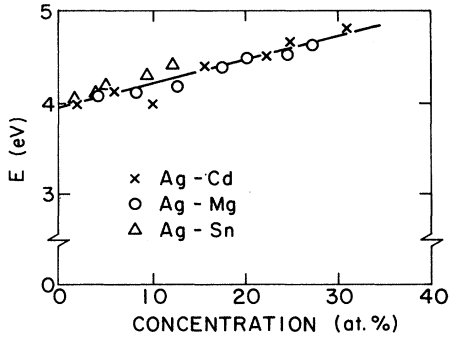

FIG. 15. Variation of the energy at which the second derivative of ϵ_2 goes through zero for the high-energy absorption as a function of atomic concentration for α-phases of some Ag-based alloys.

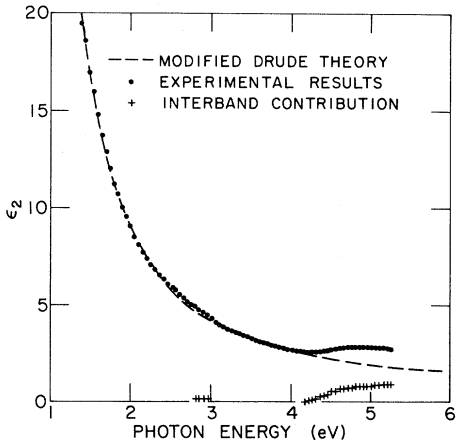

FIG. 16. Decomposition of ϵ_2 into interband and modified Drude parts for an 11.8 at.% Sn in Ag α-phase alloy.

goes through zero as a function of concentration. The variation of AgMg and AgCd is the same within experimental uncertainty. The extrapolated value for pure Ag is 3.95 ± 0.03 eV in good agreement with the results of other investigators.[9,12,14,30]

The behavior of AgSn is qualitatively quite different from that of AgMg and AgCd. No low-energy peak is visible. Any L_2'-L_1 transitions must be so badly smeared that they no longer produce any sharp structure. The behavior of AgSn in the energy region which showed Drude behavior for AgCd and AgMg is no longer Drude-like. In order to fit that data it was necessary to assume a variation of the form

$$\omega\epsilon_2 = \sigma_{D/\hbar} + \omega_p^2 \tau/(\omega^2\tau^2 + 1), \tag{7}$$

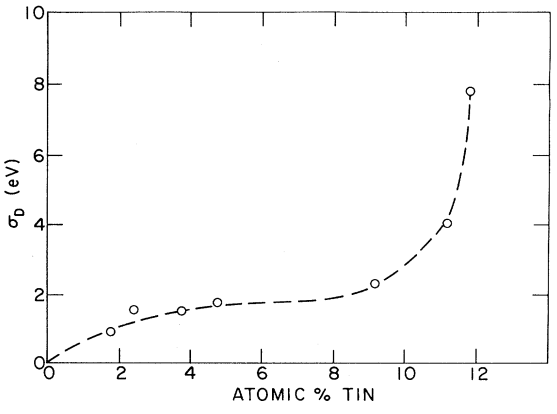

FIG. 17. Constant term σ_D in the modified Drude expression as a function of composition for AgSn α-phase alloys.

TABLE IV. Values of x^2 for various α-phase Ag alloys.

Sample	x^2
AgCd	0.22
AgMg	0.29
AgIn	0.45
AgSn	0.73
AgSb	1.07

where a constant σ_D independent of ω is added to the Drude behavior, and $\hbar$ is Planck's constant divided by 2π. A typical match of this modified Drude form to the data is shown in Fig. 16. The values of σ_D obtained by this fitting are shown in Fig. 17 and values of E_p, ϵ_1^0, and E_τ are given in Figs. 9, 10, and 11 respectively.

Only the high-energy interband absorption retains sharp structure in AgSn alloys. We plot the energy at which the second derivative of ϵ_2 goes through zero for these alloys in Fig. 15 as a function of the *atom* percentage of the Sn atoms (not the $\vec{s}$).

VI. DISCUSSION

To verify that AgMg and AgCd are class-A alloys in the vicinity of E_f, we must determine x^2 from (3) for these alloys. The real part of the energy shift $\Sigma_1(k)$ can be estimated from the shift in E_f according to the rigid band model, and $\Sigma_2(k)$ can be estimated from residual resistance measurements or phase-shift analysis.[2,3] The values determined[2,3] for x^2 are shown in Table IV. As can be seen, at E_f both AgMg and AgCd satisfy the class-A standard while AgSn is a class-B alloy.

We cannot determine directly the class of the alloy states in the vicinity of L_{4^+} and in the d bands as we can for states near E_f. Since the states near L_{4^+} have the same dominant s-p character as do the states near E_f, we expect that these states will fit in the same class as do the states near E_f. Thus, we expect that for AgMg and AgCd, the states near L_4^+ will be class A while for AgSn these will be Class B.

The d bands in all of the alloys should be class B. To understand this we note that the location of the d states in all of the three alloying elements with Ag is outside the d band of pure Ag. In such a case, theory indicates that for energies corresponding to the vicinity of the d band of pure Ag, the alloy wave functions have a "Swiss-cheese" appearance[31-34]—the wave function has near-zero amplitude around the non-Ag component. This is true for Mg with no occupied d states as it is for Cd and Sn with occupied d states. Such strong perturbation of the wave function from a Bloch form is indicative of class-B behavior.

The perturbation of the d band by the non-Ag component is approximately the same for all three alloys for the same *atomic* percent. This explains the, at first hand, surprising result that Mg and Cd perturb the alloy d band the same within experimental error even though Mg has no occupied d states while Cd does. For the same electron per atom ratio $\mathfrak{z}$ the perturbation of the d band in AgSn is less than that of AgMg and AgCd because the required atomic percent of Sn is $\frac{1}{3}$ as large.

Because the d band is class B, the description of changes in absorption induced by alloying cannot be described by direct transitions, but by indirect ones. However, the d band is so flat that there is not much difference in the energy at which transitions initiate in direct or nondirect transitions so that there is not much quantitative difference expected in the d-band absorption edge energy whether the d band is class A or class B. For sake of further discussion it is simpler to use class-A terminology in discussing the d-band absorption edge and we will do so since the quantitative difference is small.

In discussing the absorption edge of transitions from E_f to band 7, the difference between direct and indirect transitions is large. If indirect transitions are present, no absorption edge is expected. Transitions can occur at any photon energy from occupied states near E_f to any unoccupied state and there is no energy below which absorptions cannot occur as is the case for direct transitions. With indirect transitions present, transitions can occur from occupied states in band 6 to unoccupied states in the same band, something that is not allowed in direct transitions.

The dramatic difference in the absorption below 4 eV between AgMg and AgCd on one hand and AgSn on the other is explained by fact that AgMg and AgCd exhibit class-A behavior while AgSn exhibits class-B behavior. For class-A alloys, direct transitions dominate and the band structure of Fig. 8 for pure Ag can be used to qualitatively understand the absorptions. The addition of the energy shift $\Sigma_1(\vec{k})$ to the energies of pure Ag must also be accounted for in order to obtain quantitative agreement. In order for the rigid-band model to be correct, $\Sigma_1(\vec{k})$ must be independent of $\vec{k}$. For various reasons one does not expect this extreme condition to be satisfied and nonrigid distortion of the band structure of Fig. 8 is expected.

The experimental data confirm this. The results are summarized in Table V. Transitions from d band 5 to E_f in band 6 increase in energy at a slower rate than rigid-band behavior while transitions from E_f to band 7 decreases in energy at a faster rate than rigid band. The $\Sigma_1(\vec{k})$ for the alloy states in band 7 grows more negative than those at E_f by an amount of 1.0 eV per electron per atom while $\Sigma_1(\vec{k})$ for the alloy states in band 5 becomes less negative as those at E_f by an amount of 1.3 eV per electron per atom. In other words, on alloying, the bottom of band 7 lowers relative to band 6 while the top of band 5 raises relative to band 6. Similar qualitative behavior where the conduction band sinks relative to the d band is found in CuAl alloys.[35]

TABLE V. Comparison of measured variations of absorption edges and the real part of the energy shift Σ_1 with rigid-band-model values.

	Rigid band	Expt.
band-5–to–band-6 absorption edge	4.0 eV/$\Delta\mathfrak{z}$	2.7 eV/$\Delta\mathfrak{z}$
band-6–to–band-7 absorption edge	−3.63 eV/$\Delta\mathfrak{z}$	−4.68 eV/$\Delta\mathfrak{z}$
$\Sigma_1(E_f)$-$\Sigma_1(5)$	0	−1.3 eV/$\Delta\mathfrak{z}$
$\Sigma_1(7)$-$\Sigma_1(E_f)$	0	−1.0 eV/$\Delta\mathfrak{z}$

The width of the d band in pure Ag is determined by the s-d hybridization interaction and by the wave function overlap between atom sites. The contribution of the s-d interaction to the d-band width would not be greatly modified by alloying. Overlap is modified by alloying since each alloying atom acts like a vacancy as far as the d-states are concerned and decreases the number of neighbors with which overlapping can occur. In periodic solids the bandwidth is proportional to the number of overlapping neighbors which varies as $1-c$ but including the effect of disorder it is found that the decrease is significantly slower,[32] something like $(1-c)^{1/2}$.

The s-d interaction is the dominant contributor to the d bandwidth in Ag and from the above discussion we can expect that the Ag d bandwidth in the alloy will remain closely the same in the alloy. In AgSn and AgCd, new d states are added deeper in energy corresponding to the filled d states in Cd and Sn, but at the energies corresponding to d band in pure Ag, the width remains unchanged, though the density of states on average decreases by the factor $1-c$ to account for the smaller number of d states per unit volume on Ag atoms. We thus note that the relative upward movement of the top of the d band in the alloy is characteristic of the whole Ag d band.

This relative movement and decrease in weight of the Ag d band on alloying should affect the energies of the states in bands 6 and 7. Hybridization between d states raises the energy of states in band 6 and 7 with s character.[36] Thus, states at L_{4^+}, which have s character, are raised while states at L_{4^-}, which have p character, are not so affected. The d states of Cd and Sn are not very effective in this hybridization effect because they are so deep in energy while Mg has no effect because of its lack of d states. Alloying, thus, decreases the number of d states and the hybridization effect. On the other hand, the rising of the Ag d band on alloying increases the hybridization effect. However, the

net effect is a decrease in the hybridization as seen by the lowering of states near L_{4^+} relative to E_f.

Another alloying effect will change the relative energies between L_{4^+} and L_{4^-}. As alloying occurs, a given electron state changes its energy (measured by Σ_1) because it probes the changed potential at the sites of the added atoms. Measurements indicate that the potential perturbation induced by Mg, Cd, and Sn have a larger attractive p-wave interaction than s-wave interaction.[37] Thus, states near L_{4^-}, which have p character, will be lowered in energy by a larger amount than the s-character states at L_{4^+} by this direct interaction with the alloy potential. This effect is opposite from the decreased hybridization effect. The experiment shows that the decreasing hybridization is dominant and it is larger in magnitude than indicated by the relative lowering of the L_{4^+} states because of the partially cancellating effect of the direct interaction with the alloy potential.

This direct interaction with the alloy potential can also explain the relative upward movement of the alloy d states with alloying. As discussed, the states near E_f see an attractive potential from the alloy perturbation and have a negative Σ_1. However the Ag d states see essentially a strong repulsive potential near the non-Ag sites which repels the wave function. This is true for Cd and Sn as for Mg. Calculations show that the change in the average energy of a state under these circumstances is small[34] ($\Sigma_1 \approx 0$). Thus the relative change is as seen experimentally, a relative rise of the Ag d states toward E_f.

Measurements of the change in the Fermi surface neck radius in AgCd alloys are also in agreement with the decreasing hybridization effect on alloying.[4,38] It is found that the neck radius increase on alloying is less than that predicted by the rigid-band model, which indicates that the Fermi surface is becoming more spherical than the rigid band model. This result is explained by the decreasing hybridization with alloying.

In discussing AgSn we cannot simply be guided by the band structure of pure Ag as given by Fig. 8. The changes induced by alloying cannot be described in terms of E-vs-$\vec{k}$ relations. In particular indirect transitions dominate in these changes on alloying which would smear out the low-energy absorption and its sharp structure. As argued before, the d band to E_f sharp structure would still persist. The experiments strikingly confirm this picture and the class-B character of AgSn. We have no detailed theoretical understanding of class-B behavior and will not try to discuss the experimental results further.

Optical measurements on Cu-based alloys[15] also gave indications of class-A and class-B behavior and the measurements in those cases can be interpreted along the same lines as used here for the Ag-based alloys. Cu-Zn is a class-A alloy in the analogous regions as are AgMg and AgCd. Cu-Ge and Cu-As are class-B alloys. Cu-Ga appears to be an alloy in transition between class A and class B, as are AgIn and AgAl alloys as indicated by other optical measurements.[8,14]

The decreased hybridization due to the dilution of Cu atoms was proposed by Pells and Montgomery[15] in discussing their optical data and we agree with their analysis on this point. However, their analysis and that of others[8] also claim that the optical data can be compared with Friedel's theory of the motion of E_f with alloying.[39] This is not correct. The results of Friedel refer to questions of the position of E_f on an *absolute* scale and have *no* connection with *relative* energy levels as measured by optical absorption. In addition, the Friedel arguments on the change in the absolute value of E_f in concentrated alloys has been shown to be incorrect.[40]

Calculations of the band structure of α-phase CuZn by use of an average T-matrix approximation have been made.[41] Because of the relatively complicated nature of the transitions that lead to the structure in the absorptivity of Cu, the type of transitions that produce some of the varying structure with alloying is under controversy and the optical data are not able to subject the calculation to a critical check.[41] In Ag-based alloys the transitions that contribute to the absorptions are known and could be used as a critical check on any calculations of class-A alloys. Unfortunately, at the moment no such calculations exist.

It is important to note that the difference between class-A and class-B behavior is not simply a matter of electron mean-free-path considerations. Although class-A behavior corresponds to a mean free path of many lattice spacings, the inverse is not true. A long mean free path does not guarantee class-A behavior. This is illustrated by the optical data presented here. At no concentration does AgSn show the low-energy peak behavior, even at concentrations where the mean free path of the electrons is greater than in AgCd and AgMg. For example the 3.8-at.% AgSn alloy had approximately the same measured E_τ, and thus mean free path, as did the 27-at.% AgMg alloy. As can be seen in Fig. 7 the 3.8-at.% AgSn alloy showed no sign whatsoever of the low-energy peak while the 27-at.% AgMg alloy, as illustrated in Fig. 6 did show a clearly defined low-energy peak. Comparing at about the same electron per atom ratio we note that the 12.5-at.% AgMg alloy shows that a definite low-energy peak is visible at that electron per atom ratio. It is not possible to explain this difference due to smearing introduced simply by mean-free-path considerations, but the ideas of $x^2 \ll 1$ and

the forward-scattering approximation must be invoked to obtain an understanding.

VII. CONCLUSIONS AND SUMMARY

Optical measurements on the α-phase of AgMg, AgCd, and AgSn alloys show strikingly that these alloys can be classified into two classes, called A and B. Class-A alloys, where $x^2 \ll 1$, can be described by the same concepts as used for pure metals, with the added advantage of being able to change the electron per atom ratio z. The optical properties of class-A alloys are dominated by direct transitions. Class-B alloys, where $x^2 \gtrsim 1$, cannot be straightforwardly described in terms of pure material concepts. Changes in optical absorption with alloying are dominated by indirect transitions and our present theoretical knowledge is not sufficient to understand this case in detail.

Other major new experimental results of the measurements are (a) the absorption edge from transition between states near $L_2' - L_1$ occurs at 3.3 ± 0.08 eV for pure Ag; (b) the plasma frequency in the Drude region is constant within experimental error throughout the α-phase of the alloys; (c) with alloying the states in band 7 move down in energy toward the states in band 6 near E_f, relative to their values in pure Ag; (d) with alloying the states in band 5 move up in energy toward the states in band 6 near E_f, relative to their values in pure Ag; (e) AgSn alloys do not follow a Drude variation in the low-energy region while AgMg and AgCd do. A phenomenological constant σ_D must be added to the Drude term to explain the variation for AgSn.

Recent relativistic band calculations of Ag by Christensen[16] predict the initiation of the L_2'-L_1 transition at 3.37 eV in good agreement with our experimental results. The detailed shape of the L_2'-L_1 absorption as a function of energy as predicted by Christensen does not agree with our measurements but his calculation assumed constant matrix elements which presumably is in error. Previous nonrelativistic band calculations predicted the gap to be 0.86 eV greater so that the L_2'-L_1 transition would initiate within the large absorption from the d bands, in disagreement with our measurements. The value for the L_2'-L_1 gap is important because it is used in empirical fitting of pseudopotentials and setting of phase shifts of potentials.[42]

Within experimental uncertainty, no significant difference was found in the variation of the d band to E_f absorption edge energy between silver-cadmium and silver-magnesium alloys, indicating that the energy bands are similar in the two alloys to at least 5 eV below the Fermi surface. This result, which is, offhand, surprising since cadmium has occupied d states while Mg has none, is explained by theory whereby both Cd and Mg (and also Sn) repell the d states of Ag.

The nonrigid behavior of the energy levels in AgCd and AgMg alloys can be understood qualitatively in terms of our present understanding of alloys. The more detailed understanding of the behavior of AgSn alloys, as an example of class-B alloys, must await a more extensive development of alloy theory.

---

*Supported by the Air Force Office of Scientific Research. Based on the thesis of C. J. Flaten submitted as partial fullfillment for the requirement of Ph.D. degree, University of Washington, September 1972.

†Deceased.

[1]T. Muto, Sci. Pap. Inst. Phys. Chem. Res. Tokyo 34, 377 (1938); R. H. Parmenter, Phys. Rev. 97, 587 (1955); J. Friedel, Adv. Phys. 3, 446 (1954); E. A. Stern, Phys. Rev. 144, 545 (1966); V. Heine and D. Weaire, in *Solid State Physics*, edited by H. E. Ehrenreich, F. Seitz, and D. Turnball (Academic, New York, 1970), Vol. 24, pp. 427–454.

[2]E. A. Stern, Phys. Rev. B 7, 1303 (1973).

[3]E. A. Stern, Proceedings of the Michigan State University Summer School on Alloys, 1972 (unpublished), pp. 65-102.

[4]E. A. Stern, in *Charge Transfer/Electronic Structure of Alloys*, edited by R. Willens and L. Bennett (Metallurgical Society of AIME, New York, 1974), pp. 197–222.

[5]B. Velicky and K. Levin, Phys. Rev. B 2, 938 (1970).

[6](a) H. G. Liljenvall and A. G. Matthewson, J. Phys. C Suppl. 3, 341 (1970); (b) P. Winsemius, Ph.D. thesis (Rijks Universiteit Te Leiden, Leiden, Netherlands, 1973) (unpublished).

[7]E. L. Green and L. Muldawer, Phys. Rev. B 2, 330 (1970).

[8]G. B. Irani, T. Huen, and F. Wooten, Phys. Rev. B 3, 2385 (1971).

[9]C. E. Morris and D. W. Lynch, Phys. Rev. 182, 719 (1969).

[10]P. O. Nilsson and B. Sandell, Solid State Commun. 8, 721 (1970).

[11]M. Garfinkel, J. J. Tieman, and W. F. Engeler, Phys. Rev. 148, 695 (1966).

[12]B. F. Schmidt and D. W. Lynch, Phys. Rev. B 3, 4015 (1971).

[13]See, e.g., J. Rivory, Opt. Commun. 1, 53 (1969).

[14]R. M. Morgan and D. W. Lynch, Phys. Rev. 172, 628 (1968); P. O. Nilsson, Phys. Scr. 1, 189 (1970).

[15]G. P. Pells and H. Montgomery, J. Phys. C Suppl. 3, 330 (1970).

[16]N. F. Christensen, Phys. Status Solidi B 54, 551 (1972).

[17]C. J. Flaten, Ph.D. thesis (University of Washington, Seattle, Wash., 1972) (unpublished).

[18]W. B. Vail, III (private communication).

[19]R. H. Huebner, E. T. Arakawa, R. A. MacRae, and R. N. Hamm, J. Opt. Soc. Am. 54, 1434 (1960).

[20]L. G. Schulz, J. Opt. Soc. Am. 44, 357 (1958); L. G. Schulz and F. R. Tangherlini, *ibid.* 44, 362 (1958).

[21]H. Ehrenreich and H. R. Philip, Phys. Rev. 128, 1622 (1962).
[22]M. Dujardin and M. Theye, J. Phys. Chem. Solids 32, 2033 (1971).
[23]P. B. Johnson and R. W. Christy, Phys. Rev. B 6, 4370 (1972).
[24]O. Hunderi and H. P. Myers, J. Phys. F 3, 683 (1973).
[25]E. A. Stern, *Optical Properties and Electronic Structure of Metals and Alloys*, edited by F. Abeles (North-Holland, Amsterdam, 1966), p. 396.
[26]P. Dobberstein, A. Hampe, and G. Sauerbrey, Phys. Lett. A 27, 256 (1968); S. N. Jasperson and S. E. Schnatterly, Phys. Rev. 188, 759 (1969).
[27]M. Welkowsky and R. Braunstein, Solid State Commun. 9, 2139 (1971).
[28]L. Walden and T. Gustafsson, Phys. Scr. 6, 73 (1972).
[29]R. Rosei, C. H. Culp, and J. H. Weaver, Phys. Rev. B 10, 484 (1974).
[30]D. Beaglehole and E. Erlbach, Phys. Rev. B 6, 1209 (1972).
[31]E. A. Stern, Physics 1, 255 (1965); *Energy Bands in Metals and Alloys*, edited by L. H. Bennett (Gordon and Breach, New York, 1968), pp. 151–173.
[32]B. Velicky, S. Kirkpatrick, and H. Ehrenreich, Phys. Rev. 175, 747 (1968).
[33]P. Soven, Phys. Rev. 156, 809 (1967).
[34]E. A. Stern and A. Zin, Phys. Rev. B 9, 1170 (1974); A. Zin, Ph.D. thesis (University of Washington, Seattle, Wash., 1973)(unpublished).
[35]R. S. Rea and A. S. DeReggi, Phys. Rev. B 9, 3285 (1974).
[36]F. M. Mueller, Phys. Rev. 153, 659 (1967).
[37]L. C. R. Alfred and D. O. Van Ostenburg, Phys. Rev. 161, 569 (1967); L. C. R. Alfred (private communication). The x^2 for Mg is obtained from that of Cd by multiplying by the ratio of their residual resistances in Ag.
[38]W. B. Vail, III and E. A. Stern (unpublished).
[39]J. Friedel, cited in Ref. 2.
[40]E. A. Stern, Phys. Rev. B 5, 366 (1972).
[41]A. Bansil, H. Ehrenreich, L. Schwartz, and R. E. Watson, Phys. Rev. B 9, 445 (1974).
[42]B. R. Cooper, E. L. Krieger, and B. Segall, Phys. Rev. B 4, 1734 (1971).